Available online at www.sciencedirect.com

ScienceDirect

IFAC PapersOnline CONFERENCE PAPER ARCHIVE

IFAC PapersOnLine 54-8 (2021) 27–32

LPV model identification of a flapping wing MAV

Matteo Passaro * **Marco Lovera** *

* *Dipartimento di Scienze e Tecnologie Aerospaziali, Politecnico di Milano, Via La Masa 34, 20156, Milano, Italy (e-mail: marco.lovera@polimi.it).*

Abstract: The problem of model identification for the local dynamics of a flapping wing MAV is considered. Following a discussion of the underlying modelling challenges, an approach to model identification is proposed and two subspace model identification methods for LTP and LPV systems are applied and compared, with the aim of obtaining a high fidelity model of the MAV dynamics.

1. INTRODUCTION

Flapping wing micro aerial vehicles (MAVs) have received a lot of interest in the last 10 years due to the potential advantages that their peculiar method of generating lift and control action may introduce when compared to conventional quadcopters. In general, it can be foreseen that these MAVs may be better suited for indoor operation with respect to their rotary wing counterparts due to their faster response and manoeuvrability, which are essential when navigating in small spaces where obstacle avoidance is a main requirement. It must also be noticed that unlike quadcopters the class of MAVs considered in this paper does not rely entirely on conventional aerodynamics and may scale much better to miniature sized vehicles. These characteristics along with an ever increasing understanding of the fundamentals of flapping flight (see, *e.g.*, Dickinson et al. (1999) and Sun and Tang (2002)) and an evolution in micro-technology are leading to an increasing interest in the design of these kind of machines, some examples exhibiting different size scales, mechanisms and architectures being the AeroVironment Nano Hummingbird (Keennon et al. (2012)), the Delfts Delfly (De Croon et al. (2016)) and the Harvard RoboBee (Wood et al. (2013)).

While first principle modelling can be used to study the flight dynamics of flapping wing MAVs in a qualitative way, the complexity of the underlying aerodynamics calls for an experimental approach. Given the time-variability introduced by flapping, methods for model identification of linear time periodic (LTP) and linear parameter varying (LPV) systems have to be considered. The problem of identifying LTP models from data has been studied extensively in the model identification literature. Classical results have been derived in the Prediction Error Minimisation (PEM) framework (Ljung (1999)), in analogy with existing results for linear time invariant (LTI) input-output and state space models, see for example the classical reference Bittanti et al. (1994) and the references therein. Periodic extensions of AutoRegressive with eXtra input (ARX) and AutoRegressive-Moving Average with eXtra input (ARMAX) models, usually denoted, respectively, Periodic AutoRegressive with eXtra input (PARX) and Periodic AutoRegressive-Moving Average with eXtra input (PARMAX), can be defined by allowing the coefficients of the polynomials to be periodic functions of time, with integer period K. In the LTI case the PEM approach can be also applied to fixed-structure state space representations; this holds also in the LTP case, but leads to iterative optimisation schemes which might be challenging to handle.

To handle this difficulty, as well as to simplify the application of model identification to MIMO LTP systems, periodic extensions of subspace model identification methods have been developed over the last few years. Specifically, over the years many authors have developed variants of LTI Subspace Method Identification (SMI) algorithms dedicated to the identification of LTP models. Early works in this direction include the LTP extensions of the intersection algorithm of Moonen et al. (1989) (see Hench (1995)) and of the MOESP algorithm of Verhaegen (1994) (see Verhaegen and Yu (1995)) and the approach of Liu (1997). In Felici et al. (2007) an approach to LPV model identification subject to the requirement of a periodic scheduling sequence has been proposed. In recent years novel approaches to subspace identification of LTP systems have been proposed, both in the time-domain and in the frequency-domain (using the Harmonic Transfer Function (HTF)), see for example Yin and Mehr (2009); Louarroudi et al. (2012); Goos and Pintelon (2016); Wood (2011); Uyanik et al. (2019); Yin et al. (2020). Note, in passing, that in the rotorcraft industry model identification of periodic systems is currently studied with the idea in mind of developing high performance controllers for on blade control (OBC), higher-harmonic-control (HHC), load alleviation control (LAC) and individual blade control (IBC).

In view of the above discussion in this paper the problem of model identification for the local dynamics of a flapping wing MAV is considered and subspace model identification methods for LTP and LPV systems are used to obtain a control-oriented model, which is subsequently applied to control law design.

The paper is organised as follows. In Section 2 the nonlinear dynamic model of the MAV and the corresponding

2405-8963 Copyright © 2021 The Authors. This is an open access article under the CC BY-NC-ND license.
Peer review under responsibility of International Federation of Automatic Control.
10.1016/j.ifacol.2021.08.576

simulator are presented. The linearisation, averaged models and controller synthesis are presented in Section 3, the LTP identification procedure is presented in Section 4 and lastly some concluding remarks are reported in Section 5.

2. MATHEMATICAL MODEL OF THE MAV

The flapping wing MAV model considered in this paper is based on the work described in Taha et al. (2014); in the following, a concise presentation of the model is provided (the reader can refer to the cited reference for further details). In the present dynamic analysis only the rigid-body degrees of freedom are taken into account and the center of gravity (CG) inertial effect due to the wing motion was not considered. The equations of motion are written in a body frame according to the following convention: x_b pointing forward, y_b pointing to the right wing and z_b completing the triad. The present paper focuses on the longitudinal motion, hence the rigid body equations of motion resemble the ones of longitudinal motion of a conventional aircraft:

$$\begin{pmatrix} \dot{u} \\ \dot{w} \\ \dot{q} \\ \dot{\theta} \end{pmatrix} = \begin{pmatrix} -qw - g\sin\theta \\ qu + g\cos\theta \\ 0 \\ q \end{pmatrix} + \begin{pmatrix} \frac{1}{m}X \\ \frac{1}{m}Z \\ \frac{1}{I_y}M \\ 0 \end{pmatrix}, \qquad (1)$$

where g represents the gravitational acceleration; and m, I_y are, respectively, the body mass and pitching moment of inertia. The state variables are the forward velocity u, the vertical velocity w, the pitching angular velocity q and pitch angle θ. X, Z and M represent the forward and vertical forces along with pitching moment respectively. These forces will be the ones introducing the periodicity in the system, being generated by the flapping motion of the wings. The aerodynamics involved in flapping flight are very complex in nature being the flowfield unsteady and nonlinear. The main contributions that the present model takes into account are leading edge vortex, rotational effects and the effect of wake capture. The type of insect considered (Sphingidae, commonly referred as hawk moths) exhibits a stroke of the wings that is essentially in the horizontal plane, therefore the motion of the wings is described by only two angles, φ for the flapping angle and η as the angle of attack induced by the wing pitching angle:

$$\varphi(t) = \phi_0 - \Phi\cos(2\pi f t) \qquad (2)$$

$$\eta(t) = \begin{cases} \alpha_d(t), & U > 0 \\ \pi - \alpha_u(t), & U < 0, \end{cases} \qquad (3)$$

where ϕ_0 represents the zero of the flapping angle, defined so that the stroke of the wing starts from a position which is perpendicular to the body of the insect when $\phi_0 = 0$, Φ is the amplitude of the oscillation and f the frequency of wingbeat. In equation (3) the geometric angle of attack changes with the relative wind velocity $U = \sqrt{(r\dot{\varphi} + u\cos\varphi)^2 + w^2}$ where r is the distance from the hinge along the wing. This change is chosen to be a piecewise function of the flap position of the wing, being equal to α_u during the upstroke phase and α_d during the downstroke. In general these two angles are different in order to generate a pitching moment if there is an offset between CG and hinge of the wings ($x_h \neq 0$), as will be shown in the data for the study at hand the offset will be set to zero and the angles will be the same. Having $\phi_0 \neq 0$ introduces a difference between the distance traveled ahead of the hinge of the wings and the one behind, introducing an offset between it and the center of pressure averaged over one period, thus introducing a pitching moment. This will be considered in the following as the input used to introduce a change in pitching attitude or horizontal velocity of the MAV, just like longitudinal cyclic pitch in a helicopter rotor. In an analogous way Φ is controlled in a fashion similar to a collective input in order to control the heave motion of the MAV.

Once the forces and moments are written in terms of the aerodynamics as a function of the coupled body motion and flap-pitch motion of the wings equation (1) becomes:

$$\begin{pmatrix} \dot{u} \\ \dot{w} \\ \dot{q} \\ \dot{\theta} \end{pmatrix} = \begin{pmatrix} -qw - g\sin\theta \\ qu + g\cos\theta \\ 0 \\ q \end{pmatrix} + \begin{pmatrix} \frac{1}{m}X_0 \\ \frac{1}{m}Z_0 \\ \frac{1}{I_y}M_0 \\ 0 \end{pmatrix} + \begin{bmatrix} X_u & X_w & X_q & 0 \\ Z_u & Z_w & Z_q & 0 \\ M_u & M_w & M_q & 0 \\ 0 & 0 & 0 & 0 \end{bmatrix} \begin{pmatrix} u \\ w \\ q \\ \theta \end{pmatrix}. \qquad (4)$$

Most of the parameters in equation (4) are time-varying, driven by $\varphi(t)$, $\dot{\varphi}(t)$ and $\eta(t)$. The forces and moments are in fact defined as:

$$\begin{aligned} X_0 &= -2K_{21}\dot{\varphi}(t)|\dot{\varphi}(t)|\cos\varphi(t)\sin^2\eta(t) \\ Z_0 &= -K_{21}\dot{\varphi}(t)|\dot{\varphi}(t)|\sin 2\eta(t) \\ M_0 &= 2\dot{\varphi}(t)|\dot{\varphi}(t)|\sin\eta(t)\,(K_{22}\Delta x\cos\varphi(t) + K_{21}x_h\cos\eta(t) \\ &\quad + K_{31}\sin\varphi(t)\cos\eta(t)) \end{aligned} \qquad (5)$$

By default the input influences the stability derivatives through $\varphi(t)$ and $\dot{\varphi}(t)$ introducing another level of complexity. In order to simplify the model the derivatives that follow are bound to vary accordingly to the default motion of the wings and will not be influenced by variations in ϕ_0 and Φ:

$$\begin{aligned} X_u &= -4\frac{K_{11}}{m}|\dot{\varphi}(t)|\cos^2\varphi(t)\sin^2\eta(t) \\ X_w &= -\frac{K_{11}}{m}|\dot{\varphi}(t)|\cos\varphi(t)\sin 2\eta(t) \\ X_q &= \frac{K_{21}}{m}|\dot{\varphi}(t)|\sin\varphi(t)\cos\varphi(t)\sin 2\eta(t) - x_h X_w \\ Z_u &= 2X_w \\ Z_w &= -2\frac{K_{11}}{m}|\dot{\varphi}(t)|\cos^2\eta(t) \\ Z_q &= 2\frac{K_{21}}{m}|\dot{\varphi}(t)|\sin\varphi(t)\cos^2\eta(t) - \frac{K_{\mathrm{rot}_{12}}}{m}\dot{\varphi}(t)\cos\varphi(t) - x_h Z_w \\ M_u &= 4\frac{K_{12}\Delta x}{I_y}|\dot{\varphi}(t)|\cos^2\varphi(t)\sin\eta(t) + \frac{m}{I_y}(2X_q - x_h Z_u) \\ M_w &= 2\frac{K_{12}\Delta x}{I_y}|\dot{\varphi}(t)|\cos\varphi(t)\cos\eta(t) + 2\frac{K_{21}}{I_y}|\dot{\varphi}(t)|\sin\varphi(t)\cos^2\eta(t) + \\ &\quad - \frac{m x_h}{I_y}Z_w \end{aligned} \qquad (6)$$

$$
\begin{aligned}
M_q = &-\frac{2\Delta x}{I_y}|\dot{\varphi}(t)|\cos\varphi(t)\cos\eta(t)\left(K_{12}x_h + K_{22}\sin\varphi(t)\right)\\
&+\frac{1}{I_y}\dot{\varphi}(t)\cos\varphi(t)\left(K_{\mathrm{rot}_{13}}\Delta x\cos\varphi(t)\cos\eta(t) + K_{\mathrm{rot}_{22}}\sin\varphi(t)\right)+\\
&-\frac{2}{I_y}|\dot{\varphi}(t)|\cos^2\eta(t)\sin\varphi(t)\left(K_{21}x_h + K_{31}\sin\varphi(t)\right)+\\
&-\frac{K_v\mu_1 f}{I_y}\cos^2\varphi(t) - \frac{mx_h}{I_y}Z_q.
\end{aligned}
\tag{7}
$$

The constant coefficients which appear in the above expressions for the derivatives, and which derive from the integrals performed to obtain lift and moments, are defined as:

$$
\begin{aligned}
K_{mn} &= \frac{1}{2}\rho A I_{mn}\\
I_{mn} &= 2\int_0^R r^m c^n(r)\mathrm{d}r\\
K_{\mathrm{rot}_{mn}} &= \pi\rho\left(\frac{1}{2}-\Delta x\right)I_{mn}\\
K_v &= \frac{\pi}{16}\rho I_{04}
\end{aligned}
\tag{8}
$$

Where $c(r)$ is the chord distribution along the wingspan and r is the distance from the hinge. The operational geometric angles of attack on the wings are computed by imposing the average lifting force equal to the weight of the MAV as shown in the following equation:

$$
\alpha_d = \alpha_u = \frac{1}{2}\sin^{-1}\left(\frac{mgT^2}{\pi^2\rho A I_{21}\Phi^2}\right), \tag{9}
$$

with A computed as:

$$
A = \frac{\pi AR}{2\left[1+\sqrt{\left(\frac{\pi AR}{a_0}\right)^2+1}\right]}, \tag{10}
$$

where T is the flapping period equal to the inverse of f and AR is the aspect ratio computed as R^2/S.

In Table (1) the data used to describe the MAV are reported. Some known morphological parameter (namely $\bar{c}$, $\hat{r}_1$ and $\hat{r}_2$) are reported and are used to fit a sufficiently accurate $c(r)$, refer to the original paper for the procedure.

3. LINEARIZATION AND AVERAGING

The system described in the previous section is a nonlinear time periodic (NLTP) system that is found from direct simulation to be unstable in hover due to lack of pitch stiffness. Therefore it is necessary to design a controller to make it closed loop stable. The chosen procedure for stabilization is the design of a linear quadratic (LQ) controller using the averaged system dynamics (see, *e.g.*, Khalil (2001)). To this purpose the following operations must be performed in sequence:

(1) linearization of the system around an unknown periodic orbit;
(2) averaging along the period of flap;
(3) discretization of the obtained system.

Table 1. Data from Taha et al. (2020).

Parameter	Value	Comment
f	26 Hz	flapping frequency
Φ	58°	flapping amplitude
R	51.8 mm	semi-wingspan
$\bar{c}$	18.94 mm	mean chord
S	947.8 mm^2	surface area of one wing
$\hat{r}_1$	0.43	ad. first moment of area
$\hat{r}_2$	0.499	ad. second moment of area
m	1.32 g	mass
I_y	3.36 $g\cdot cm^2$	pitch inertia moment
x_h	0	ad. offset between hinge and CG
ρ	1.225 kg/m^3	air density
g	9.81 m/s^2	gravitational acceleration
μ_1	0.2	viscosity coefficient
ϕ_0	0°	mean flapping angle
a_0	2π	2-D lift curve slope
$\Delta\hat{x}$	0.05	chord ad. offset between pitch axis and center of pressure

In principle the orbit around which the linearization is performed should be known, but as a first guess an orbit coincident with the origin was chosen aiming at a perfect hover (null velocity, pitch angle and pitch rate). The adopted approach has been to iterate among the design of the controller ($K_{LQ}^{(k)}$) and the simulation and linearisation of the nonlinear closed-loop system, repeating the process to obtain $K_{LQ}^{(k+1)}$. In order to perform operation (1) a numerical differentiation scheme was implemented which leveraged the centred differences method on the NLTP system written in the form $f(\dot{x},x,u)=0$, to give

$$
\begin{aligned}
A_i &= \frac{\partial f}{\partial x}\Big|_i = \frac{f(\dot{\overline{x}},\overline{x}+h_i,\overline{u}) - f(\dot{\overline{x}},\overline{x}-h_i,\overline{u})}{2h}\\
B_i &= \frac{\partial f}{\partial u}\Big|_i = \frac{f(\dot{\overline{x}},\overline{x},\overline{u}+h_i) - f(\dot{\overline{x}},\overline{x},\overline{u}-h_i)}{2h},
\end{aligned}
\tag{11}
$$

where h is the perturbation magnitude, h_i is the perturbation of the i-th state or input written as $h_i=[0,...,h,...,0]'$ with h being at the i-th position, $\dot{\overline{x}}$, $\overline{x}$ and $\overline{u}$ are the state derivative, the state and the input at trim respectively. Each state or input is perturbed individually in order to obtain a matrix of derivatives by assembling the A_i columns. Once this operation is performed for all the n states the A_k matrix is obtained where k is the k-th step in the period. Repeating the process for all samples in the period the final result should be:

$$
\begin{aligned}
A = &\Big[[A_1A_2...A_i...A_n]_1 \quad ... \quad [A_1A_2...A_i...A_n]_k\\
&... \quad [A_1A_2...A_i...A_n]_P\Big] \quad \in\mathbb{R}^{(n,nP)}\\
B = &\Big[[B_1B_2...B_i...B_r]_1 \quad ... \quad [B_1B_2...B_i...B_r]_k\\
&... \quad [B_1B_2...B_i...B_r]_P\Big] \quad \in\mathbb{R}^{(n,rP)},
\end{aligned}
\tag{12}
$$

where P is the number of samples in one period, n is the number of states and r is the number of inputs. The obtained system is an LTP in the state space form $\dot{x}=A_kx+B_ku$. The averaging step consisted simply in the averaging over the P samples of one period of the A_k and

B_k matrices, obtaining $A_{avg} \in \mathbb{R}^{(n,n)}$ and $B_{avg} \in \mathbb{R}^{(n,r)}$. The linearized averaged system can now be discretized using one of the many methods available, for the present analysis forward differences were used.

$$\begin{aligned} A^d_{avg} &= I_{n,n} + T_s A_{avg} \\ B^d_{avg} &= T_s B_{avg}, \end{aligned} \tag{13}$$

where T_s is the timestep, $I_{n,n}$ is the n-th order identity matrix and the superscript d denotes that the matrices refer to a discrete system.

3.1 LQ regulator design

The above-described procedure was performed once despite the first controller performance were already satisfactory, in order execute the linearization on the true orbit and obtain a linearized model describing truly the real NLTP system. Thus one iteration was performed, meaning that the controller used will be $K^{(2)}_{LQ}$. The obtained $K \in \mathbb{R}^{(r,n)}$, constructed by expressing $K^{(2)}_{LQ}$ in the form of equation (12) is used to write the closed-loop system depicted in Figure 1, in which also an exogenous disturbance e is added on the input which will be used for the identification in the following section.

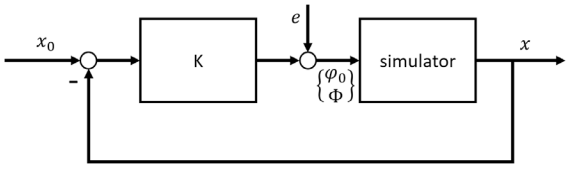

Fig. 1. Closed-loop system with exogenous input.

4. LPV MODEL IDENTIFICATION

The system derived in the previous section is now used to perform an LTP identification, with the aim of obtaining an accurate model of the system useful for controller synthesis purposes. The methods used in the present analysis are of the subspace type, the reason behind this choice being their robustness and non-iterative nature. The I/O sequence used for the identification is given by the open-loop inputs (ϕ_0 and Φ) and the state variables (u, w, q and θ).

4.1 Overview of the identification algorithms

Two methods are used and compared in the present analysis, namely the periodic intersection algorithm of Hench (1995), and the periodic PBSID algorithm proposed in Van Wingerden et al. (2009). The latter has the additional requirement of knowing the scheduling sequence μ_k which describes the evolution of the parameters of the system during the period as,

$$A_k = \sum_{i=1}^{m} A^{(i)} \mu_k^{(i)}, \tag{14}$$

where m represents the number of LPV system matrices. In the same manner also B_k, C_k, and D_k are defined. In this formalism the LPV system matrices are $A^{(i)} \in \mathbb{R}^{n \times n}$, $B^{(i)} \in \mathbb{R}^{n \times r}$, $C^{(i)} \in \mathbb{R}^{\ell \times n}$ and $D^{(i)} \in \mathbb{R}^{\ell \times r}$ and can be regarded as blocks to be weighted by the scheduling sequence $\mu_k = \left(\mu_k^{(1)} \mu_k^{(2)} \cdots \mu_k^{(m)}\right)^{\mathrm{T}}$ in order to reconstruct the time varying system matrices A_k, B_k, C_k and D_k. The scheduling sequence for the system at hand has been found though spectral analysis of the time history of the coefficients of the linearized system. The actual procedure used the results of a fast fourier transform (FFT) to reconstruct the coefficients of the sines and cosines that summed would give an acceptable fit of the parameters. A comparison between the non-parametric and parametric models for the derivatives is illustrated in Figure 2. The coefficients, once reassembled, would constitute the LPV system matrices, and the sines and cosines at multiples of the flap frequency the scheduling parameters.

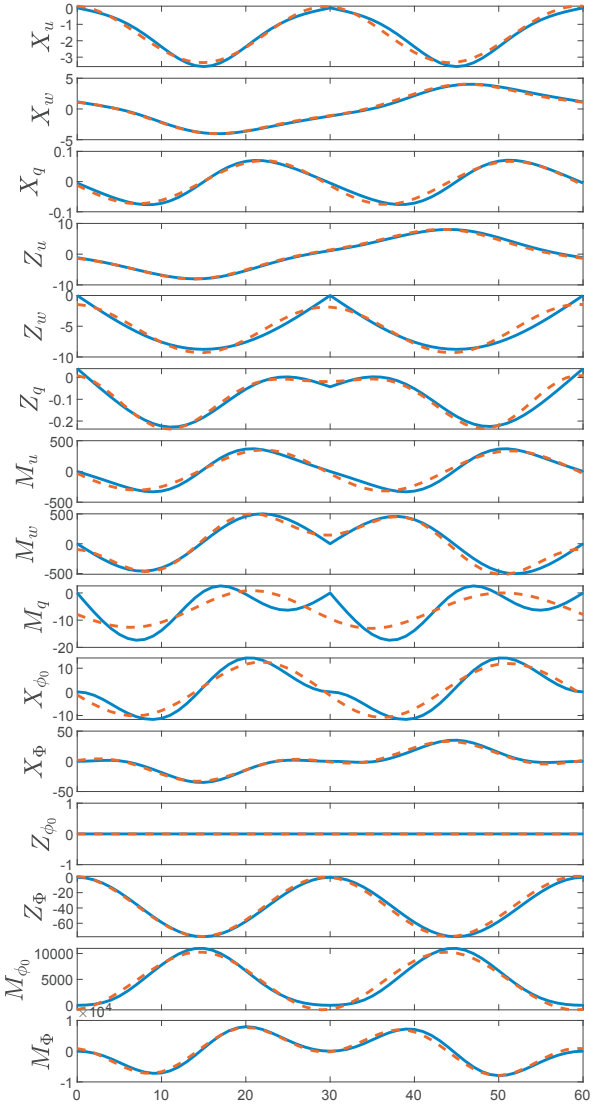

Fig. 2. Comparison between the original (blue lines) and the scheduled coefficients (dashed red lines) using $P = 60$.

The Fourier series approximation was stopped at $m = 7$, *i.e.*, the expansions include the mean value and the cosine and sine parts of the harmonics at f, $2f$ and $3f$.

4.2 Design of identification experiments

In order to design an informative input for the identification of the system, the dominant frequencies of the system are inspected by looking at the eigenvalues. From this analysis the maximum frequency is found to be $3.64Hz$. From an analysis of the difference between the response of the linear and nonlinear systems to the same input it is found that some kind of nonlinear distortion is present. In order to mitigate this effect, multisines were chosen as input (Schoukens and Ljung (2019)).

$$e(t) = \sum_{k=1}^{F} U_k \sin\left(2\pi k f_0 t + \varphi_k\right), \tag{15}$$

where the chosen fundamental frequency f_0 is $0.5Hz$, the harmonics used are nine ($F = 9$), the amplitude U_k is of $0.1deg$ for the odd harmonics and $0deg$ for the even ones and the phase φ_k is always set as zero. The validation is performed by exciting the system in closed-loop with a sweep sequence on both input channels. The signals span linearly from $0.5rad/s$ to $5rad/s$ with amplitude equal to $0.1deg$.

4.3 Identification and validation results

The identification of the NLTP system is carried out in closed-loop being the plant unstable. The system is excited with the exogenous input $e(t)$ (see Figure 1) and the time history of the states is simulated (x_{pert}), then, knowing the controller, the perturbation and the states the real input entering the plant is reconstructed (u_{pert}). This operation is also performed with a non perturbed system in order to reconstruct the trimmed states and input (x_{trim} and u_{trim}). Lastly, the time histories that are fed to the identification algorithms are the difference between the two results: $u_{id} = u_{pert} - u_{trim}$ and $x_{id} = x_{pert} - x_{trim}$. In Figure 3 the identification results of the intersection algorithm with window size $i = 2$ are reported and in Figure 4 the same is done for the PBSID algorithm with past and future windows $p = f = 3$. The corresponding validation results are reported in Figure 5 and Figure 6, respectively. Furthermore, in order to assess quantitavely the performance of the models the Variance Accounted For (VAF) is provided in Table 2.

Table 2. VAF of the results

Identification				
	u	w	q	θ
Hench	64.45%	95.37%	61.25%	0%
van Wingerden *et al.*	89.32%	99.24%	67.16%	73.89%
Validation				
	u	w	q	θ
Hench	0%	60.06%	61.58%	0%
van Wingerden *et al.*	74.48%	98.97%	73.73%	37.41%

As can be seen from the results both methods provide models which are in good qualitative agreement with the simulated data. Table 2 however clearly shows that the LTP model obtained using the intersection algorithm is not able to capture the dynamic response of some of the variables, with very poor performance on the attitude response on the identification dataset and both attitude and forward speed on the validation dataset. The LPV model obtained using the PBSID, on the other hand, is capable of providing a satisfactory performance. This increment in performance is due to the increased robustness given by the presence of the scheduling sequence, which constraints how the coefficients evolve.

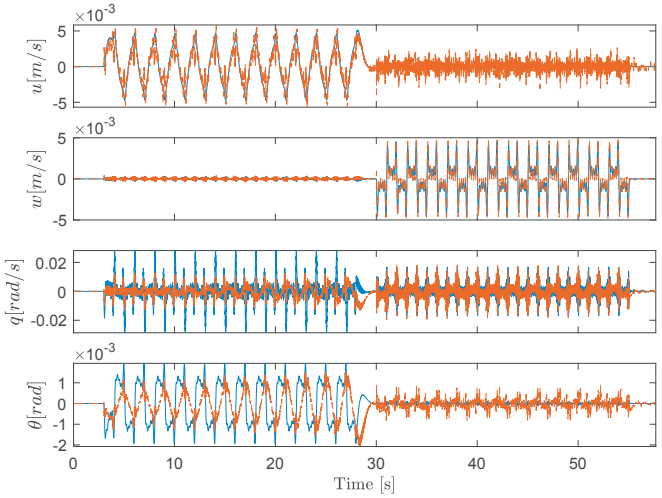

Fig. 3. Identification results of the Hench algorithm (dashed red lines) compared to nonlinear simulation (blue lines).

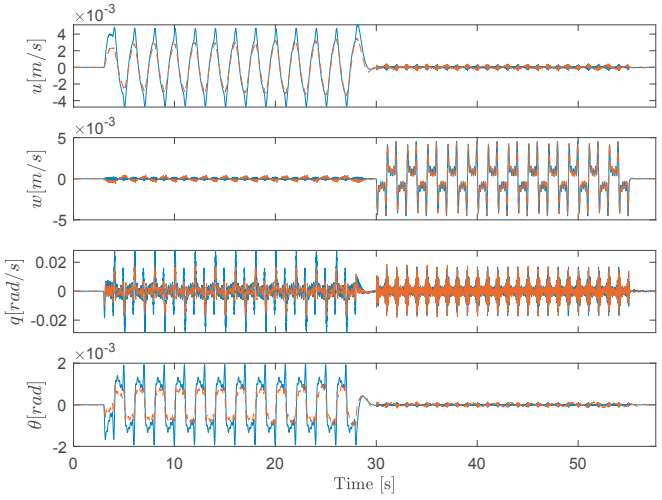

Fig. 4. Identification results of the van Wingerden *et al.* algorithm (dashed red lines) compared to nonlinear simulation (blue lines).

5. CONCLUSION

The problem of model identification for the dynamics of a flapping wing MAV has been considered. A simulation model, based on the dynamic formulation of Taha et al. (2014) has been developed and employed as a starting point to develop an approach to the execution of simulated experiments. Two algorithms, one for LTP and one for LPV model identification have been compared and the latter has been shown to be adequate to face the complexity of the task. Future work will aim at studying the problem of experiment design and nonlinear distortions minimization for the dynamics of flapping wing MAVs.

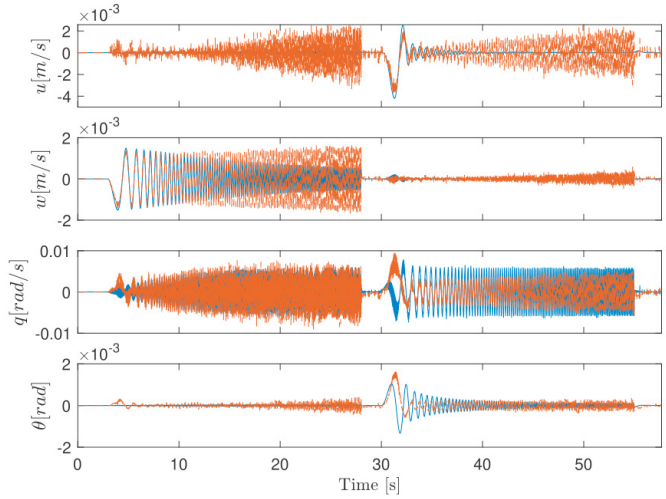

Fig. 5. Validation results of the Hench algorithm (dashed red lines) compared to nonlinear simulation (blue lines).

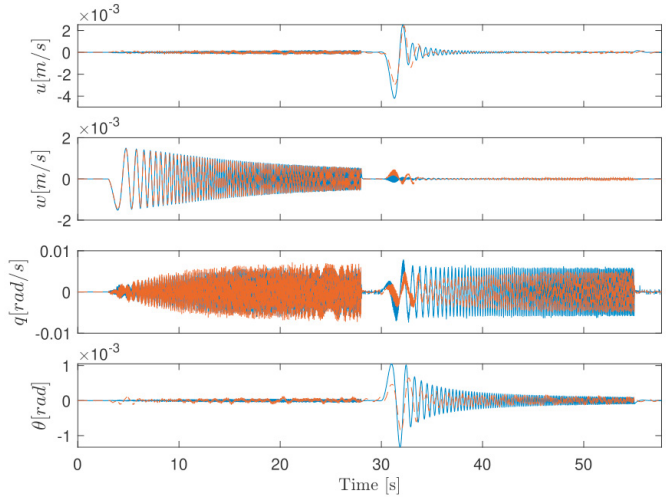

Fig. 6. Validation results of the van Wingerden *et al.* algorithm (dashed red lines) compared to nonlinear simulation (blue lines).

REFERENCES

Bittanti, S., Bolzern, P., De Nicolao, G., and Piroddi, L. (1994). Representation, prediction and identification of cyclostationary processes - a state space approach. In W. Gardner (ed.), *Cyclostationarity*, chapter 5, 267–294. IEEE Press.

De Croon, G., Perçin, M., Remes, B., Ruijsink, R., and De Wagter, C. (2016). The delfly. *Dordrecht: Springer Netherlands. doi*, 10, 978–94.

Dickinson, M.H., Lehmann, F.O., and Sane, S.P. (1999). Wing rotation and the aerodynamic basis of insect flight. *Science*, 284(5422), 1954–1960.

Felici, F., van Wingerden, J., and Verhaegen, M. (2007). Subspace identification of MIMO LPV systems using a periodic scheduling sequence. *Automatica*, 43(10), 1684–1697.

Goos, J. and Pintelon, R. (2016). Continuous-time identification of periodically parameter-varying state space models. *Automatica*, 71, 254–263.

Hench, J. (1995). A technique for the identification of linear periodic state space models. *International Journal of Control*, 62(2), 289–301.

Keennon, M., Klingebiel, K., and Won, H. (2012). Development of the nano hummingbird: A tailless flapping wing micro air vehicle. In *50th AIAA aerospace sciences meeting including the new horizons forum and aerospace exposition*, 588.

Khalil, H. (2001). *Nonlinear systems, 3rd Edition*. Prentice Hall.

Liu, K. (1997). Identification of linear time-varying systems. *Journal of Sound and Vibration*, 206(4), 487–505.

Ljung, L. (1999). *System Identification: Theory for the User*. Prentice Hall.

Louarroudi, E., Pintelon, R., and Lataire, J. (2012). Nonparametric tracking of the time-varying dynamics of weakly nonlinear periodically time-varying systems using periodic inputs. *IEEE Transactions on Instrumentation and Measurement*, 61(5), 1384–1394.

Moonen, M., De Moor, B., and Vandewalle, J. (1989). On- and off-line identification of linear state-space models. *International Journal of Control*, 49(1), 219–232.

Schoukens, J. and Ljung, L. (2019). Nonlinear system identification: A user-oriented road map. *IEEE Control Systems Magazine*, 39(6), 28–99.

Sun, M. and Tang, J. (2002). Unsteady aerodynamic force generation by a model fruit fly wing in flapping motion. *Journal of experimental biology*, 205(1), 55–70.

Taha, H.E., Hajj, M.R., and Nayfeh, A.H. (2014). Longitudinal flight dynamics of hovering mavs/insects. *Journal of Guidance, Control, and Dynamics*, 37(3), 970–979.

Taha, H.E., Kiani, M., Hedrick, T.L., and Greeter, J.S. (2020). Vibrational control: A hidden stabilization mechanism in insect flight. *Science Robotics*, 5(46), eabb1502–eabb1502.

Uyanik, I., Saranli, U., Ankarali, M., Cowan, N., and Morgul, O. (2019). Frequency-domain subspace identification of linear time-periodic (ltp) systems. *IEEE Transactions on Automatic Control*, 64(6), 2529–2536.

Van Wingerden, J., Houtzager, I., Felici, F., and Verhaegen, M. (2009). Closed-loop identification of the time-varying dynamics of variable-speed wind turbines. *International Journal of Robust and Nonlinear Control: IFAC-Affiliated Journal*, 19(1), 4–21.

Verhaegen, M. (1994). Identification of the deterministic part of MIMO state space models given in innovations form from input-output data. *Automatica*, 30(1), 61–74.

Verhaegen, M. and Yu, X. (1995). A class of subspace model identification algorithms to identify periodically and arbitrarily time-varying systems. *Automatica*, 31(2), 201–261.

Wood, R., Nagpal, R., and Wei, G.Y. (2013). Flight of the robobees. *Scientific American*, 308(3), 60–65.

Wood, T.A. (2011). *Model-Based Flight Control of Kites for Wind Power Generation*. Ph.D. thesis, ETH Zurich.

Yin, M., Iannelli, A., Khosravi, M., Parsi, A., and Smith, R.S. (2020). Linear time-periodic system identification with grouped atomic norm regularization. *arXiv*, arXiv:2003.06653v2 [eess.SY], 289–301.

Yin, W. and Mehr, A. (2009). Identification of linear periodically time-varying systems using periodic sequences. In *Proceedings of the 2009 IEEE International Conference on Control Applications*.